# Optoelectronic performance optimization for transparent conductive layers based on randomly arranged silver nanorods

**Mikita Marus,[1] Aliaksandr Hubarevich,[1] Hong Wang,[1] Aliaksandr Smirnov,[2] Xiaowei Sun,[1,3] and Weijun Fan[1,*]**

[1]*School of Electrical and Electronic Engineering, Nanyang Technological University, 50 Nanyang Avenue, 639798, Singapore*

[2]*Department of Micro- and Nano-Electronics, Belarusian State University of Informatics and Radioelectronics, 6 P. Brovki, Minsk, 220013, Belarus*

[3]*EXWSUN@ntu.edu.sg*

[*]*EWJFAN@ntu.edu.sg*

**Abstract:** Optoelectronic performance of transparent conductive layers (TCLs) based on randomly arranged silver (*Ag*) nanorods (NRs) is simulated. Models for calculation of optical and electronic properties were proposed founded on finite-difference time-domain method and percolation theory respectively. Obtained simulation results are well conformed to experimental data. The influence of angle deviation of NR crossings on the transmittance and sheet resistance are demonstrated. The balance between transmittance and sheet resistance which can be easily set by varying the combinations of NR radius and NR number is shown. Our results demonstrate that randomly arranged *Ag* layers are promising candidates for flexible TCLs.



**OCIS codes:** (130.0250) Optoelectronics; (240.0310) Thin films; (240.6680) Surface plasmons.

## References and links

1. S. Xie, Z. Ouyang, B. Jia, and M. Gu, "Large-size, high-uniformity, random silver nanowire networks as transparent electrodes for crystalline silicon wafer solar cells," Opt. Express **21**(S3 Suppl 3), A355–A362 (2013).
2. A. K. Kumar, C. W. Bae, L. Piao, and S.-H. Kim, "Silver nanowire based flexible electrodes with improved properties: High conductivity, transparency, adhesion and low haze," Mater. Res. Bull. **48**(8), 2944–2949 (2013).
3. J. van de Groep, P. Spinelli, and A. Polman, "Transparent conducting silver nanowire networks," Nano Lett. **12**(6), 3138–3144 (2012).
4. B. Han, Y. Huang, R. Li, Q. Peng, J. Luo, K. Pei, A. Herczynski, K. Kempa, Z. Ren, and J. Gao, "Bio-inspired networks for optoelectronic applications," Nat Commun **5**, 5674 (2014).
5. M. Aryal, J. Geddes, O. Seitz, J. Wassei, I. McMackin, and B. Kobrin, "16.1: Sub-Micron Transparent Metal Mesh Conductor for Touch Screen Displays," in *SID Symposium Digest of Technical Papers* (Wiley Online Library, 2014), pp. 194–196.
6. C. R. Martin, "Membrane-based synthesis of nanomaterials," Chem. Mater. **8**(8), 1739–1746 (1996).
7. C. L. Haynes and R. P. Van Duyne, "Nanosphere lithography: a versatile nanofabrication tool for studies of size-dependent nanoparticle optics," J. Phys. Chem. B **105**(24), 5599–5611 (2001).
8. M. E. Stewart, C. R. Anderton, L. B. Thompson, J. Maria, S. K. Gray, J. A. Rogers, and R. G. Nuzzo, "Nanostructured plasmonic sensors," Chem. Rev. **108**(2), 494–521 (2008).
9. S.-E. Kim, Y.-H. Han, B. Lee, and J.-C. Lee, "One-pot fabrication of various silver nanostructures on substrates using electron beam irradiation," Nanotechnology **21**(7), 075302 (2010).
10. A. Tao, P. Sinsermsuksakul, and P. Yang, "Polyhedral silver nanocrystals with distinct scattering signatures," Angew. Chem. Int. Ed. Engl. **45**(28), 4597–4601 (2006).
11. T. Ito and S. Okazaki, "Pushing the limits of lithography," Nature **406**(6799), 1027–1031 (2000).
12. B. L. Cushing, V. L. Kolesnichenko, and C. J. O'Connor, "Recent advances in the liquid-phase syntheses of inorganic nanoparticles," Chem. Rev. **104**(9), 3893–3946 (2004).
13. Y. Sun and Y. Xia, "Shape-controlled synthesis of gold and silver nanoparticles," Science **298**(5601), 2176–2179 (2002).
14. K. Chen, L. Tang, Y. Xia, and Y. Wang, "Silver(I)-Coordinated Organogel-Templated Fabrication of 3D Networks of Polymer Nanotubes," Langmuir **24**(24), 13838–13841 (2008).

#232121 - $15.00 USD Received 13 Jan 2015; revised 24 Feb 2015; accepted 25 Feb 2015; published 27 Feb 2015

15. C. Yang, H. Gu, W. Lin, M. M. Yuen, C. P. Wong, M. Xiong, and B. Gao, "Silver nanowires: from scalable synthesis to recyclable foldable electronics," Adv. Mater. **23**(27), 3052–3056 (2011).
16. Lumerical FDTD Solutions, *https://www.lumerical.com/tcad-products/fdtd/*.
17. B. Last and D. Thouless, "Percolation theory and electrical conductivity," Phys. Rev. Lett. **27**(25), 1719–1721 (1971).
18. Q. G. Du, K. Sathiyamoorthy, L. P. Zhang, H. V. Demir, C. H. Kam, and X. W. Sun, "A two-dimensional nanopatterned thin metallic transparent conductor with high transparency from the ultraviolet to the infrared," Appl. Phys. Lett. **101**(18), 181112 (2012).

## 1. Introduction

Metallic nanorod meshes made themselves to be promising alternative to indium tin oxide (ITO) transparent conductive layers [1–4]. Latest experimental results show that optoelectronic parameters of such meshes can reach values of up to 95% transmittance at 3 Ohm/sq sheet resistance [5]. Main factors influencing on optoelectronic performance are material, shape, dimension, density and arrangement of rods. Randomly arranged silver nanorod meshes are currently prevailing due to their fabrication simplicity and low cost. Chemical, template-directed or lithographic methods are used for NR preparation; while spin, Meyer rod, dip, spray and others coating methods are applied for NR deposition [6–15]. Cylindrically shaped NRs of 30, 60 and 90 nm diameter and 15-40 μm length are typically implemented within experimental studies [1–3]. Unfortunately, the total period of the research of random NR meshes was increased by long calculation time due to large simulation unit cell area. Application of new generation supercomputers can decrease this process duration down to few months. With the use of the supercomputer we managed to obtain full theoretical investigation of optoelectronic performance of randomly arranged *Ag* NR mesh within visible wavelength range. In result, trade-off between transmittance and sheet resistance as well as influence of NR crossing angle on optoelectronic performance were investigated for various rod diameters and their densities. Moreover, the distinction between randomly and uniformly arranged NRs was demonstrated.

## 2. Methodology

The optical properties were simulated using the finite-difference time-domain method (FDTD) which is commercially available within Lumerical software [16]. The incident light is distributed along *Z* axis. The simulation area was narrowed to unit cell. Its size along *X* and *Y* axes was set to inter-rod distance *a* in case of uniformly arranged NR mesh, while for meshes with random NR arrangement these area was taken as 10 × 10 μm. Moreover, the simulation of randomly arranged ones was performed three times for arbitrarily chosen unit cell position in means of verifying the reproducibility of mesh model properties. The periodic boundary conditions and perfectly matched layers were applied parallel and perpendicularly to *Z* axis correspondingly. Mesh size for metallic layer was set to 10, 10 and 5 nm in *X*, *Y*, and *Z* directions, respectively.

The sheet resistance is calculated by percolation model from refs [17, 18]. According to this model the sheet resistance is given by:

$$R_{sh} = \frac{1}{h\sigma_0 \left(\phi_f - \phi_{crit}\right)^t}, \tag{1}$$

where $\sigma_0$ is the conductivity of metal, $\phi_f$ is the volume fraction of patterned metal layer, $\phi_{crit}$ is the volume fraction threshold when the conductivity of patterned metal layer is zero, $h$ is the thickness of the metal layer and $t$ is the critical exponent.

## 3. Results and discussion

Figure 1 demonstrates a geometrical model for distribution of uniformly (a) and randomly (b, c) arranged NRs along *X*-*Y* plane. Whole NR bunch is lying on glass substrate within same

#232121 - $15.00 USD Received 13 Jan 2015; revised 24 Feb 2015; accepted 25 Feb 2015; published 27 Feb 2015

plane perpendicular to $Z$ axis. Uniformly arranged NRs cross with each other at angle $\alpha = 90°$ and have $i$ horizontal by $j$ vertical NR configuration with inter-rod distance $a$. Each NR in randomly arranged mesh was subjected to following procedures to resemble experimental results in [1]: 1) arbitrarily shifted along $X$ and $Y$ axes for distance ranging from −1/5 to 1/5 of rod length; 2) arbitrarily tilted along $X$ and $Y$ axes for angle $\alpha_d$ ranging from −90 to 90°.

The difference of $\phi_f$ and $\phi_{crit}$ for randomly arranged NRs:

$$\phi_f - \phi_{crit} = \frac{\left(\left\langle N_i^* \right\rangle - N_{crit}\right)V_c}{V_{uc}}, \tag{2}$$

where $\left\langle N_i^* \right\rangle$, $N_{crit}$, $V_c$ and $V_{uc}$ are the effective number of NR crossings, the critical number of NR crossings required for conduction appearance, the NR crossings volume and the unit cell volume, respectively. It should be mentioned that conduction of NR mesh happens if there is at least *one* NR crossing. In our simulations with random mesh the effective NR crossing number $\left\langle N_i^* \right\rangle$ is varied from 17 to 717 and, thus, the critical NR crossing number $N_{crit}$ is negligible and can be ignored. Figures 2 (a) and 2 (b) show the calculated distribution of $\left\langle N_i^* \right\rangle$ value for 4 by 4 and 9 by 9 NR configurations, i.e. total of 8 and 18 NRs accordingly. The average quantity $\left\langle N_i^* \right\rangle$ is: 6% larger than its value for uniformly arranged NR amount $N$.

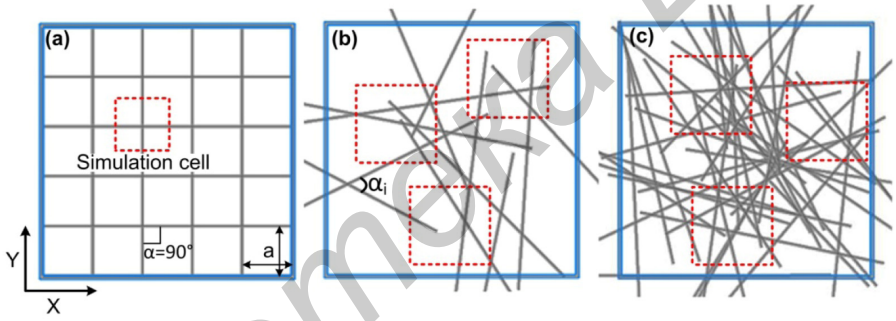


Fig. 1. Geometrical model for distribution of uniformly (a) and randomly (b, c) arranged NRs along X-Y plane, where (b) and (c) differ by NR density. Red rectangles are unit simulation cells equal to $a^2$ and 10 × 10 μm for uniform and random NRs, respectively.

Crossings volume $V_c$ for randomly arranged NRs:

$$V_c = \pi r^2 \left\langle l_i^* \right\rangle, \tag{3}$$

where, $r$ and $\left\langle l_i^* \right\rangle$ are NR radius and the effective length of NR crossings respectively. Figure 2(c) illustrates the calculation model of $\left\langle l_i^* \right\rangle$. According to this model:

$$l_i^* = \frac{2r}{\left\langle \sin(\alpha_i) \right\rangle}, \tag{4}$$

where $\alpha_i$ is angle of NR crossing. As can be seen in Fig. 2 (d), the average value of $\left\langle \sin(\alpha_i) \right\rangle$ is: 0.647. Taking into consideration Eqs. (1)–(4), the sheet resistance is modified to the following equation:

#232121 - $15.00 USD Received 13 Jan 2015; revised 24 Feb 2015; accepted 25 Feb 2015; published 27 Feb 2015

$$R_{sh} = \frac{1}{h\sigma_0}\left(\frac{V_{uc}\times 0.647}{1.06\times 2\times \pi r^3 N}\right)^t = \frac{1}{h\sigma_0}\left(\frac{V_{uc}}{3.277\times \pi r^3 N}\right)^t. \quad (5)$$

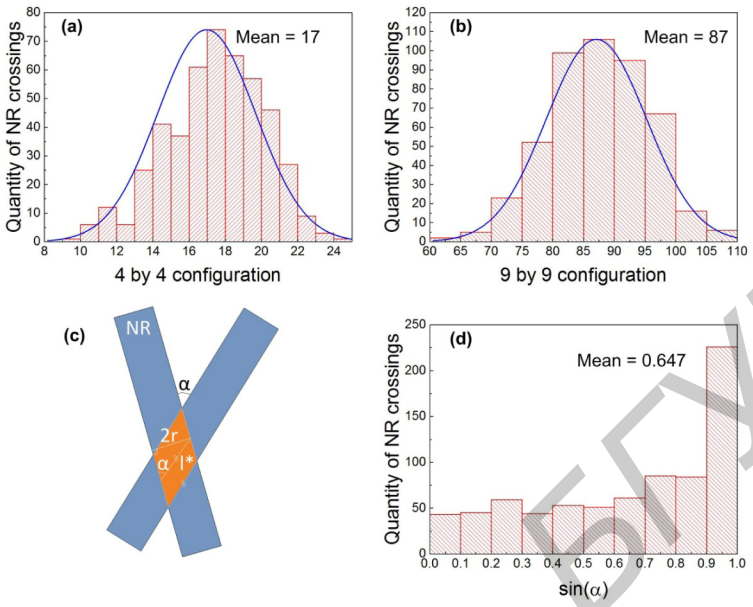


Fig. 2. Calculated values of effective NR crossings number $\langle N_i^* \rangle$ (a, b) and NR crossings effective length $\langle l_i^* \rangle$ (c, d).

Figure 3 shows the dependency of transmittance versus wavelength for different surface coverage of randomly arranged NRs with 50 nm radius. The value of critical exponent can be varied from 1 to 2 according to ref [17]. We believe that the critical exponent *t* depends on the NR mesh annealing process, i.e. NR mesh annealing *time* and *temperature*, and can significantly change the sheet resistance. We have taken $t = 1.01$ to satisfy the experimental data from ref [1]. Figure 3(a) illustrates the experimental results taken from ref [1]. while the simulated ones demonstrated in Fig. 3(b) were calculated using the above mentioned model. As can be seen, the simulated values for transmittance and sheet resistance are in good agreement with experimental data. An uniform broadband transmittance is observed for

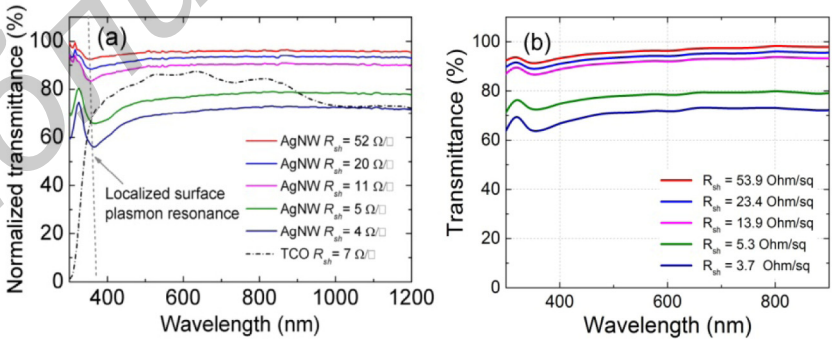


Fig. 3. Transmittance versus wavelength dependency for different surface coverage of randomly arranged NRs. (a) Experimental results reprinted with permission from ref [1]. Copyright [2011] The Optical Society. (b) Simulated results by FDTD and percolation models.

#232121 - $15.00 USD Received 13 Jan 2015; revised 24 Feb 2015; accepted 25 Feb 2015; published 27 Feb 2015

wavelengths longer than 400 nm, while decrement due to the localized surface plasmon resonance is in range of 325-400 nm.

Figure 4(a) illustrates the optical properties of NR grid for the absolute value of the angle deviation $|\alpha_d|$ ranged from 0 to 90°, where $\alpha_d = 0$ and $\alpha_d > 0$ are for uniformly and randomly arranged NRs respectively as shown in Figs. 1(a) and 1(b). The values of NR radius $r$ and surface coverage were 50 nm and 35%. Two regions of transmittance can be emphasized: (*1*) $0 < |\alpha_d| \leq 40$ and (*2*) $40 < |\alpha_d| \leq 90$. The highest transmittance of 80-85% is observed for 440-700 nm in the first region. At the same time, the considerable transmittance decrement for ranges of 325-400 and 740-900 nm is provoked by absorbance and reflectance increments respectively. The peaks of transmittance are disappearing after 400 nm and its smoothening is observed due to breaking of lattice constant periodicity. The influence of NR radius $r$ on their optical parameters is demonstrated in Fig. 4(b). The values of the absolute value of the NR angle deviation $|\alpha_d|$ and surface coverage were 90° and 35% respectively. The transmittance is varying slightly up to $r = 35$ nm, while 30% decrement is observed for

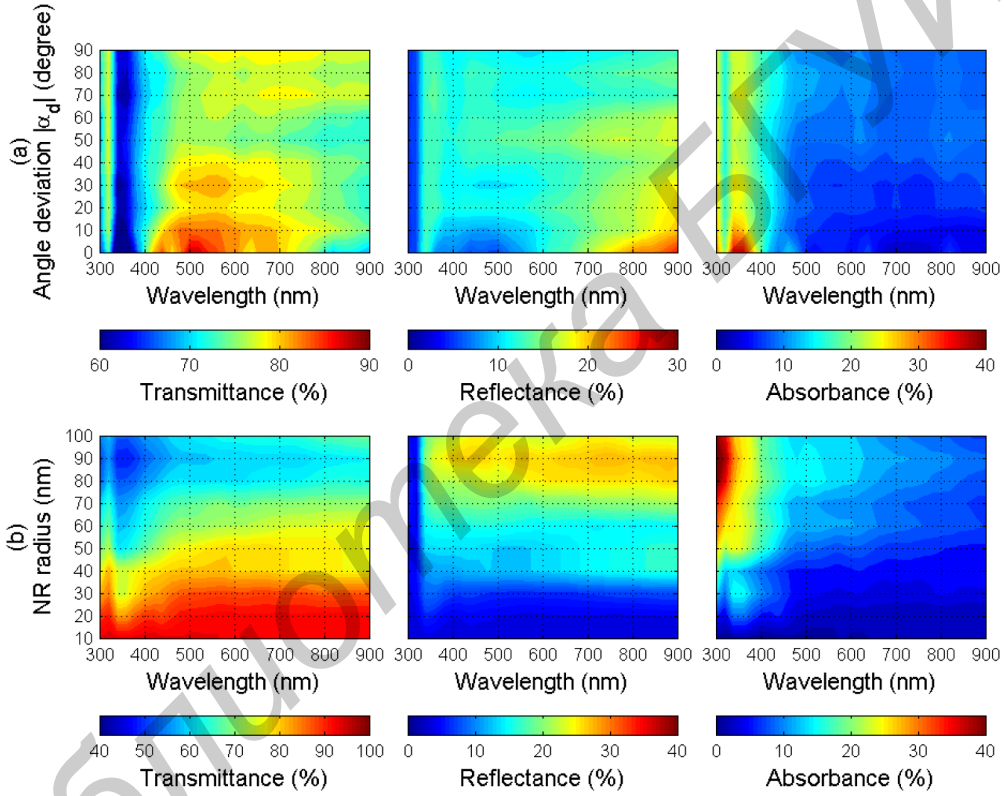


Fig. 4. (a) Influence of angle deviation $|\alpha_d|$ on optical properties of NR grid. The NR radius $r$ and surface coverage parameters are 50 nm and 35%, respectively. (b) Influence of NR radius $r$ on optical properties of NR grid. The NR angle deviation absolute value $|\alpha_d|$ and surface coverage parameters are 90° and 35% respectively.

$r \geq 35$ nm. The above mentioned drop is mainly induced by 30% increment of absorbance and reflectance in ranges of 300-400 and 400-700 nm, respectively.

Figure 5 shows the dependency of NR radius $r$ ranged from 10 to 100 nm and NR number ranged from 4 to 26 NRs on the average transmittance in visible wavelength range (left) and sheet resistance (right). Varying combinations of NR radius and NR number allows to easily find the trade-off for optoelectronic applications in terms of transmittance and sheet



#232121 - $15.00 USD Received 13 Jan 2015; revised 24 Feb 2015; accepted 25 Feb 2015; published 27 Feb 2015

resistance. For example, the transmittance of: 90% and sheet resistance of: 10 Ohm/sq, which is attractive for TCLs, can be obtained at NR number / NR radius = 6 / 60 or 14 / 30 or 24 / 20. Further optoelectronic performance improvement can be achieved by the optimizing of *Ag* NR annealing process to decrease the sheet resistance. In case of simulation the model should be modified for the critical exponent *t* in Eq. (4) to include the parameters of annealing time and temperature.

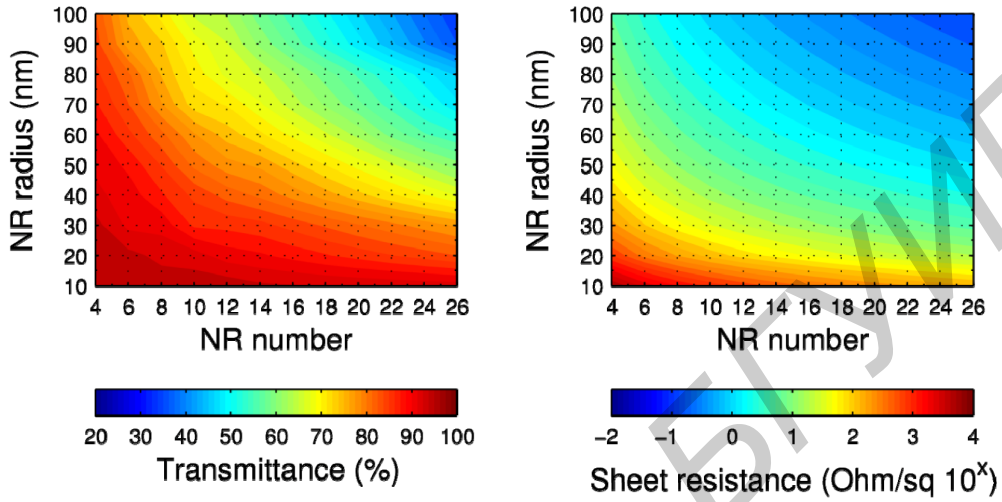


Fig. 5. Influence of NR radius r and NR number on the average transmittance in visible wavelength range (left) and sheet resistance (right).

### 3. Conclusion

Optoelectronic performances of randomly arranged *Ag* NRs are simulated and studied. Calculation models for optical and electronic properties were proposed based on the finite-difference time-domain method and percolation theory respectively. Obtained simulation results are well conformed to the experimental ones. The influence of angle deviation of NR crossings on the transmittance and sheet resistance is demonstrated. The balance between transmittance and sheet resistance of randomly arranged *Ag* NRs is shown. Our results demonstrate that randomly arranged *Ag* layers are very promising candidates for optoelectronic applications, especially for flexible TCLs.


### Acknowledgment

This project is supported by National Research Foundation of Singapore (No. NRF-CRP11-2012-01).




#232121 - $15.00 USD Received 13 Jan 2015; revised 24 Feb 2015; accepted 25 Feb 2015; published 27 Feb 2015